

Characterization of Two Mutations in the SPTLC1 Subunit of Serine Palmitoyltransferase Associated with Hereditary Sensory and Autonomic Neuropathy Type I



Annelies Rotthier^{1,2}, Anke Penno^{3,4}, Bernd Rautenstrauss^{5,6}, Michaela Auer-Grumbach⁷, Georg M. Stettner⁸, Bob Asselbergh^{1,2}, Kim Van Hoof^{1,2}, Heinrich Sticht⁹, Nicolas Lévy^{10,11}, Vincent Timmerman^{1,2}, Thorsten Hornemann^{3,12,#}, and Katrien Janssens^{1,2,#}

¹ Peripheral Neuropathy Group, VIB Department of Molecular Genetics, University of Antwerp, Antwerpen, Belgium; ² Laboratory of Neurogenetics, Institute Born-Bunge, University of Antwerp, Antwerpen, Belgium; ³ Institute for Clinical Chemistry, University Hospital Zürich, Zürich, Switzerland; ⁴ Competence Center for Systems Physiology and Metabolic Diseases, Zürich, Switzerland; ⁵ Medical Genetics Center, München, Germany; ⁶ Friedrich-Baur Institute, Ludwig Maximilian University, München, Germany; ⁷ Department of Internal Medicine, Division of Endocrinology and Nuclear Medicine, Medical University of Graz, Graz, Austria; ⁸ Department of Pediatrics and Pediatric Neurology, Georg August University, Göttingen, Germany; ⁹ Emil-Fischer-Zentrum, Institute of Biochemistry, Friedrich-Alexander University, Erlangen, Germany; ¹⁰ AP-HM, Département de Génétique Médicale, Laboratoire de Génétique Moléculaire, Hôpital d'enfants de la Timone, Marseille, France; ¹¹ Inserm UMR_S 910 : Génétique Médicale et Génomique Fonctionnelle, Faculté de Médecine de Marseille, Université de la Méditerranée, Marseille, France; ¹² Institute of Physiology and Zürich Center for Integrative Human Physiology (ZIHP), University of Zürich, Zürich, Switzerland;

#These authors contributed equally

*Correspondence to Prof. Dr. Vincent Timmerman, PhD; Peripheral Neuropathy Group, VIB Department of Molecular Genetics; University of Antwerp, Universiteitsplein 1, B-2610 Antwerpen, Belgium. Fax: +32-3-265.10.12, Tel: +32-3-265.10.24. E-mail: vincent.timmerman@molgen.vib-ua.be

Communicated by Andreas Gal

ABSTRACT: Hereditary sensory and autonomic neuropathy type I (HSAN-I) is an axonal peripheral neuropathy leading to progressive distal sensory loss and severe ulcerations. Mutations in *SPTLC1* and *SPTLC2*, encoding the two subunits of serine palmitoyltransferase (SPT), the enzyme catalyzing the first and rate-limiting step in the *de novo* synthesis of sphingolipids, have been reported to cause HSAN-I. Here, we demonstrate that the *SPTLC1* mutations p.S331F and p.A352V result in a reduction of SPT activity *in vitro* and are associated with increased levels of the deoxysphingoid bases 1-deoxy-sphinganine and 1-deoxymethyl-sphinganine in patients' plasma samples. Stably expressing p.S331F-SPTLC1 HEK293T cell lines likewise show accumulation of deoxysphingoid bases, but this accumulation is not observed in HEK293T cells overexpressing p.A352V-SPTLC1. These results confirm that the increased formation of deoxysphingoid bases is a key feature for HSAN-I as it is associated with all pathogenic *SPTLC1* and *SPTLC2* mutations reported so far, but also warrant for caution in the interpretation of *in vitro* data. ©2011 Wiley-Liss, Inc.

KEY WORDS: HSAN-I; *SPTLC1*; serine palmitoyltransferase; 1-deoxy-sphinganine

Received 14 October 2010; accepted revised manuscript 31 January 2011.

© 2011 WILEY-LISS, INC.

DOI: 10.1002/humu.21481

INTRODUCTION

Inherited peripheral neuropathies are common neurodegenerative disorders of the peripheral nervous system. They are genetically and clinically heterogeneous, but based on the predominant involvement of motor or sensory neurons, they fall into three main subclasses: hereditary motor and sensory neuropathies (HMSN), hereditary motor neuropathies (HMN) and hereditary sensory and autonomic neuropathies (HSAN). The clinical spectrum of HSAN is wide and led to the further subdivision into six subtypes (Dyck et al., 1993). Patients with hereditary sensory and autonomic neuropathy type I (HSAN-I; MIM# 162400) present with progressive loss of pain and temperature sensation in the limbs, variable distal muscle weakness and limited autonomic dysfunction. Typically, first symptoms appear between the second and third decade of life. The loss of sensation leads to painless injuries complicated by ulcerations and osteomyelitis, often necessitating amputation (Auer-Grumbach et al., 2003). HSAN-I has a dominant mode of inheritance and is associated with mutations in *SPTLC1* (MIM# 605712) (Bejaoui et al., 2001; Dawkins et al., 2001; Rotthier et al., 2009) and *SPTLC2* (MIM# 605713) (Rotthier et al., 2010), two subunits of the enzyme serine palmitoyltransferase (SPT). SPT is located at the outer membrane of the endoplasmic reticulum (ER), where it catalyzes the pyridoxal-5'-phosphate (PLP) dependent condensation of L-serine with palmitoyl-CoA. This is the first and rate-limiting step in the *de novo* biosynthesis of sphingolipids (Hanada, 2003). Sphingolipids, having both a structural and a signaling function, are essential for all eukaryotic cells. Mutations in various enzymes of the sphingolipid metabolism are associated with neurodegenerative diseases (Kolter and Sandhoff, 2006), highlighting the importance of these ubiquitous components in neuronal functioning.

A common feature of the HSAN-I associated mutations in *SPTLC1* and *SPTLC2* is a reduction of the canonical enzymatic activity, but the effect on total sphingolipid levels remains controversial (Bejaoui et al., 2001; Dawkins et al., 2001; Dedov et al., 2004; Hornemann et al., 2007). Furthermore, the mutations cause a shift in the substrate specificity of SPT, enabling the mutant enzyme to metabolize, besides serine, also alanine and glycine. This results in the formation of the two atypical deoxysphingoid bases (DSB) 1-deoxy-sphinganine (1-deoxy-SA) and 1-deoxymethyl-sphinganine (1-deoxymethyl-SA) (Zitomer et al., 2009; Gable et al., 2010; Penno et al., 2010). Both metabolites can be converted to 1-deoxy(methyl)-ceramide and 1-deoxy(methyl)-sphingosine (1-deoxy(methyl)-SO) but because they lack an essential hydroxyl group, conversion to more complex sphingolipids like glyco- or phosphosphingolipids and phosphorylation are hampered, resulting in the accumulation of these intermediate metabolites in the cell. Importantly, it was previously shown that DSBs have pronounced neurotoxic effects on neurite formation in cultured sensory neurons (Penno et al., 2010).

Recently, we performed a systematic screening of the known HSAN genes in a large cohort of HSAN patients and identified two novel *SPTLC1* mutations, p.S331F and p.A352V (Rotthier et al., 2009), bringing the total number of *SPTLC1* mutations to six (the others being p.C133W, p.C133Y, p.C133R and p.V144D) (Bejaoui et al., 2001; Dawkins et al., 2001; Rautenstrauss et al., 2009). The p.S331F mutation occurred *de novo* in a patient with a severe congenital phenotype, the p.A352V mutation was detected in an isolated patient with a typical HSAN-I phenotype. Further evaluation of the pathogenicity of this latter variant is warranted because of the absence of DNA of family members for segregation analysis, the limited evolutionary conservation of the targeted amino acid and the similar chemical properties of alanine and valine.

In the present study, we report the identification of the p.S331F mutation in a patient with severe and early-onset HSAN-I. Furthermore, functional characterization of both the p.S331F and p.A352V mutations was undertaken to a) identify differences between the p.S331F and previously described *SPTLC1* mutant proteins that could explain the severe phenotype associated with the p.S331F mutation and b) assess the pathogenicity of the p.A352V mutation.

MATERIALS AND METHODS

Subjects

Patient II.2 (MGZ-48522; Fig. 1a) has been described in Huehne et al., 2008. Patients CMT-791.01 and CMT-186.05 have been described in Rotthier et al., 2009.

Mutation analysis

After DNA extraction from EDTA blood using the Flexigene kit (Qiagen, Hilden, Germany), standard PCR and direct sequencing with ABI PRISM 3100 Avant (Big Dye v1.1, Applied Biosystems, Foster City, USA) covering all 15 coding exons and the flanking regions of the *SPTLC1* gene (GenBank: NM_178324.1) was performed. Primer sequences are available upon request. Nucleotide numbering reflects cDNA numbering with +1 corresponding to the A of the ATG translation initiation codon in the reference sequence. The initiation codon is codon 1.

Cloning

The SPTLC1 cDNA was amplified and cloned into the Gateway® entry vector pDONR221 (Invitrogen, Carlsbad, USA) using the primers SPTLC1_attb1 and SPTLC1_attb2. The *SPTLC1* mutations p.C133W, p.S331F and p.A352V were introduced by site-directed mutagenesis, using the primers listed in Supp. Table S1. The constructs were recombined in the destination vector pEF5/FRT/V5-DEST (Invitrogen), fusing the cDNA with a C-terminal V5-tag. Additionally, C-terminally EGFP-tagged constructs were constructed and recombined in the destination vector pLenti6/V5-DEST (Invitrogen). All constructs were validated by sequencing.

Stable expression of SPTLC1 constructs in HEK293T cells

Stable cell lines expressing wild type (wt) or mutant SPTLC1 were generated via calcium phosphate based transfection of the Flp-in host cell line HEK293T following manufacturer's instructions (Invitrogen). The Flp-in system ensures the stable insertion of a single copy of the transgene at a specific location. In this way, moderate and equal expression of the different transgenes is obtained.

Lymphoblastoid cell lines

Lymphoblastoid cell lines were generated as described previously in Rotthier et al., 2010.

Cell culture material and conditions

HEK293T Flp-in cells were cultivated in DMEM supplemented with 10% fetal bovine serum, 2 mM L-glutamine and 100 µg/ml penicillin/streptomycin. SH-SY5Y neuronal cells were cultured in MEM supplemented with 10% fetal bovine serum, 2 mM glutamine, 1% non-essential amino acids and 100 µg/ml penicillin/streptomycin. Lymphoblastoid cell lines were cultured in RPMI1640 medium supplemented with 10% fetal bovine serum, 2 mM L-glutamine, 1mM sodium pyruvate and 200 units/ml penicillin/streptomycin. All cells were cultivated at 37°C and 5% CO₂. All cell culture media and supplements were from Invitrogen.

In vitro SPT activity

SPT activity was measured using the radioactivity-based assay described by Rützi et al., 2009.

Fumonisin B1 block assay, lipid extraction and hydrolysis and LC-MS

These assays were performed as described in Penno et al., 2010.

Structure modelling

The structure of human SPT was modelled using the high-resolution crystal structure of the *Spingomonas paucimobilis* SPT homodimer (PDB code: 2JG2; Yard et al., 2007) as a template. The two subunits of heterodimeric human SPT exhibit a sequence similarity of respectively 47% and 50% to the bacterial template. Model building was performed using Modeller 6.2 (Sanchez and Sali, 2000) and included also the PLP cofactor covalently bound as an aldimine to K379 of SPTLC2. The resulting model was refined by energy minimization with Sybyl7.3 (Tripos Inc., St-Louis, USA). Model validation with WHATCHECK (Hooft et al., 1996) revealed a correct local geometry and no steric clashes. Rasmol (Sayle and Milner-White, 1995) was used for structure analysis and visualization.

Statistics

The two-tailed unpaired Student's t-test and the ANOVA with post hoc correction were used for statistical analysis. Error bars (standard deviation) and p-values (Student's t-test) were calculated based on three independent experiments.

RESULTS

Identification of the *SPTLC1* mutation p.S331F in a HSAN-I patient

Mutation analysis of the complete coding region of the *SPTLC1* gene in patient MGZ-48522 (II.2 in Fig. 1a), with a severe and early-onset HSAN with additional juvenile cataract and retinal detachment, led to the identification of the heterozygous missense mutation c.992C>T (p.S331F). This mutation is absent in the parents (Fig 1a) as well as in 300 control individuals. Mutations in *PMP22*, *MPZ*, *GJB1*, *EGR2*, *MFN2*, *NTRK1* and *NGF* had been previously excluded (Huehne et al., 2008). The identification of the p.S331F mutation in this patient provides additional genetic evidence for the pathogenicity of this variant, that was previously identified in patient CMT-791.01 with an atypically severe HSAN-I phenotype (Rotthier et al., 2009). The c.1055C>T (p.A352V) mutation was previously described in patient CMT-186.05 with a typical HSAN-I phenotype (Rotthier et al., 2009).

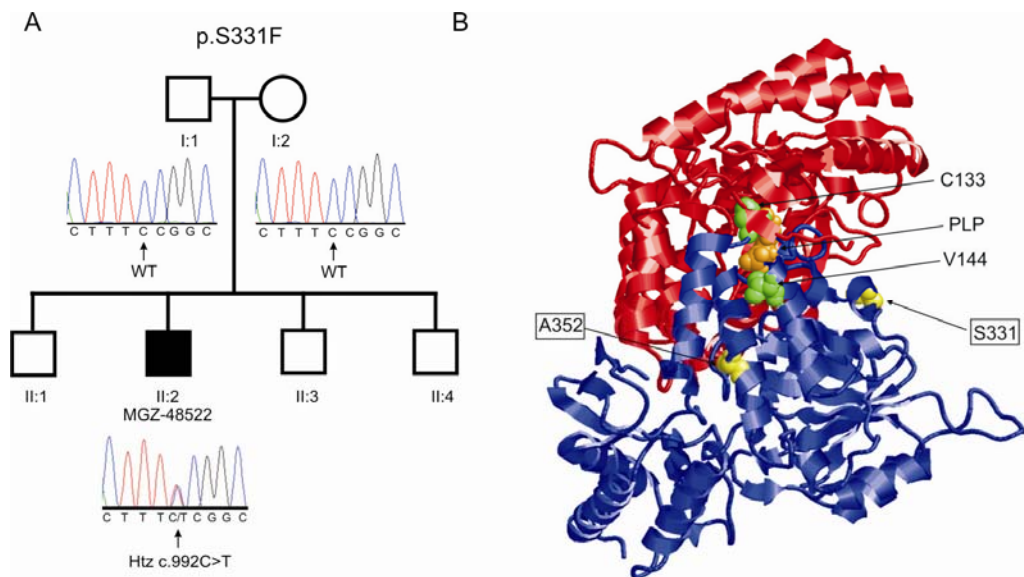


Figure 1. *De novo* p.S331F mutation in a HSAN-I patient and structural model of human SPT. (A) Pedigree of the HSAN-I patient MGZ-48522 carrying the *de novo* c.992C>T mutation (p.S331F) in *SPTLC1*, with sequence trace files of the mutation. Nucleotide numbering reflects cDNA numbering with +1 corresponding to the A of the ATG translation initiation codon in the reference sequence. The initiation codon is codon 1. (B) Structure model of the human SPT heterodimer (PDB ID: 2JGT) with the subunits represented in red and blue. The amino acids highlighted in yellow, p.S331 and p.A352, are subject of study in this report. The amino acids highlighted in green, p.C133 and p.V144, are also mutated in HSAN-I. The cofactor PLP is indicated in orange.

p.S331F and p.A352V mutant proteins have a reduced SPT activity

Complementary to genetic evidence, proof of the pathogenicity of a sequence variant can be inferred from its effect on protein function. Therefore, functional characterization of the p.S331F and p.A352V mutant proteins in stably transfected HEK293T cells was undertaken. Equal expression of the mutant proteins in HEK293 cells was confirmed by Western Blot analysis (Supp. Figure S1). First, we investigated the effect of the p.S331F and

p.A352V mutations on the canonical SPT activity using two different methods. In a first assay, *in vitro* SPT activity was determined in cell lysates by measuring the incorporation of ^{14}C labeled L-serine into lipids. SPT activity in wt SPTLC1 expressing cells was slightly different from control cells, however this difference was not observed in an alternative assay (see below). The previously characterized p.C133W mutant caused a more than 50% reduction in SPT activity which is in agreement with earlier reports (Bejaoui et al., 2002; Hornemann et al., 2007; Hornemann et al., 2009). SPT activity was reduced to a similar extent in cells expressing the mutant proteins p.S331F (35-55% reduction) and p.A352V (60-65% reduction) (Fig 2a).

In an alternative assay, growing cells were treated with Fumonisin B1 to block the sphingolipid pathway downstream of SPT. This results in a time dependent accumulation of SA. Since SPT catalyzes the rate-limiting step in the sphingolipid biosynthesis pathway, the amount of SA accumulating over time reflects canonical SPT activity. No difference in SPT activity was observed between wt SPTLC1 and control cells whereas the stable expression of the mutants resulted in a significant reduction of SA accumulation (Fig 2b). This confirms that, like the p.C133W mutant, the p.S331F and p.A352V mutations in SPTLC1 lead to a reduced SPT activity.

Like wt SPTLC1 protein, the two mutant forms of SPTLC1 colocalized with the ER marker calreticulin in SH-SY5Y neuroblastoma cells (Supp. Figure S2), rendering it unlikely that mislocalization of the mutant protein causes the loss in SPT activity.

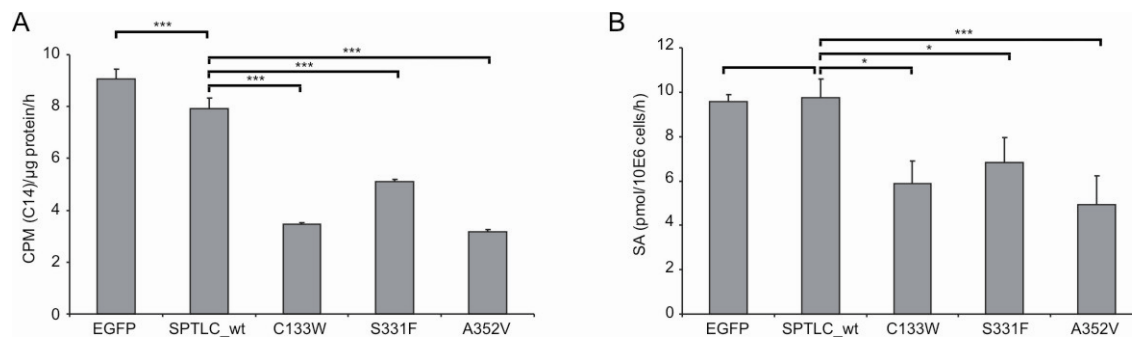


Figure 2. SPT activity in cells stably expressing SPTLC1 mutant proteins. (A) Radioactive SPT activity assay. Total cell lysate was incubated with L-serine, Palmitoyl-CoA, PLP and L-[U- ^{14}C] serine. After 60 min, lipids were extracted and the incorporation of radioactive serine was determined as a measure for SPT activity. (B) Fumonisin B1 block assay. SPT activity in HEK293T cells stably expressing wt or mutant SPTLC1 was analyzed by measuring SA accumulation after treatment with Fumonisin B1. For both experiments, EGFP expressing cells served as control. Data is represented as a mean with error bars representing standard deviations. Standard deviation was calculated based on six (A) and three (B) independent experiments. CPM: counts per minute; SA: sphinganine; *: p-value < 0.01; ***: p-value < 0.005.

Accumulation of 1-deoxysphingoid bases in p.S331F but not in p.A352V expressing HEK cells

To assess the effect of the observed reduction in SPT activity on total sphingolipid levels, we subsequently compared the sphingoid base profile of HEK293T cells expressing wt or mutant SPTLC1. We subjected the extracted total lipid fraction to a combined acid-base hydrolysis reaction; the resulting free sphingoid bases, which reflect the total amount of extracted sphingolipids, were analyzed by LC-MS. For both the HEK293T cell lines expressing the transgenic proteins and the lymphoblast cell lines of patients and controls, no significant differences in total SO levels between mutant and control cell lines could be observed (Fig 3a and 3b), indicating that despite of a reduced canonical SPT activity, total sphingolipid levels are not altered.

We furthermore analyzed the DSBs 1-deoxy-SA/1-deoxy-SO and 1-deoxymethyl-SA/1-deoxymethyl-SO, which have been shown to accumulate in cells expressing the previously characterized HSAN-I mutants and reflect the ability of the mutant proteins to use respectively alanine and glycine instead of serine as a substrate for the enzymatic reaction (Penno et al., 2010; Rothier et al., 2010). In the HEK293T cells stably expressing wt SPTLC1, the amount of 1-deoxy-SA was similar to control cells; 1-deoxy-SO was below the detection limit in these cell lines (Fig 3c). Expression of the p.C133W mutant resulted in highly elevated 1-deoxy-SA and 1-deoxy-SO formation compared to wt SPTLC1 expressing cells, in accordance with previous observations (Penno et al., 2010). The p.S331F mutant also showed significantly higher levels of 1-deoxy-SA and 1-deoxy-SO compared to

wt SPTLC1 expressing cells (p-value < 0.001). However, there was no statistical difference between the levels in the p.S331F expressing cells and in the p.C133W expressing cells. In the p.A352V expressing cells, the level of 1-deoxy-SA was similar to the level measured in wt cells; 1-deoxy-SO was above the detection limit, but low.

1-deoxysphingoid bases are elevated in biosamples of p.S331F and p.A352V patients

Interestingly, analysis of plasma samples from all three patients described in this study (the two p.S331F patients and the p.A352V patient) showed significantly elevated plasma levels of 1-deoxy-SA and 1-deoxy-SO when compared to unaffected family members of MGZ-48522 (II.2 in Fig 1a) or unrelated healthy controls (Fig 3e). In addition, levels of 1-deoxymethyl-SA and 1-deoxymethyl-SO were increased in the p.S331F patients' plasma samples, but were not detected in the plasma of the p.A352V patient. This indicates that the p.S331F mutant protein, but not the p.A352V mutant protein, is able to metabolise not only alanine, but also glycine as an alternative substrate.

Highly elevated DSB levels were also observed in lymphoblast cells of the p.S331F patient CMT-791.01 (Fig 3d). Unfortunately, no lymphoblast cell lines were available from the patient carrying the p.A352V mutation or from the p.S331F patient MGZ-48522. Levels of 1-deoxymethyl-SA and 1-deoxymethyl-SO were below the detection limit in HEK293T cells and in lymphoblast cell lines (data not shown).

Taken together, our data show that p.S331F and p.A352V mutant SPTLC1 are associated with a reduction of SPT activity *in vitro* without affecting total sphingolipid levels. Furthermore, both mutations are associated with elevated DSB levels in patients' plasma samples. For the p.S331F mutation, this finding corroborates the accumulation of DSBs found in two *in vitro* assays. For the p.A352V mutation, the result challenges the unaltered DSB formation observed *in vitro*.

DISCUSSION

Recently, we identified two novel HSAN associated sequence variants in *SPTLC1*, namely p.S331F and p.A352V (Rotthier et al., 2009). These variants are located far downstream of the 12 amino acid region clustering all other previously reported *SPTLC1* mutations (p.C133W, p.C133Y, p.C133R and p.V144D). Structural information based on a model for human SPT (Fig 1b) indicates that the C133 and V144 residues are located close to the SPTLC1:SPTLC2 dimer interface, while the S331 and the A352 amino acids are located more distally. This could imply that the pathomechanism is different for these two groups of mutations. Moreover, both the p.S331F and the p.A352V mutation were detected in a single patient (*de novo* or isolated case), providing limited genetic evidence for their pathogenicity and calling for a more in-depth analysis of their effect on protein function.

We now were able to identify a second unrelated HSAN-I patient with the p.S331F mutation (MGZ-48552; II.2 in Fig 1a), which strengthens the genetic evidence that this variant is causative. Both patients carrying the p.S331F mutation show an unusually severe phenotype with early onset insensitivity to pain and pronounced motor impairment (Table 1) and non-typical HSAN-I features. In addition to the classical symptoms, the new patient described in this study presented with juvenile cataract and retinal detachment whereas the previously reported p.S331F patient showed severe growth and mental retardation, vocal cord paralysis and gastro-oesophageal reflux. Whether these features are related to the p.S331F mutation is uncertain since most of them are atypical for HSAN-I, although some have been associated with other inherited peripheral neuropathies (Indo et al., 1996; Kok et al., 2003; Aboussouan et al., 2007; Claeys et al., 2009).

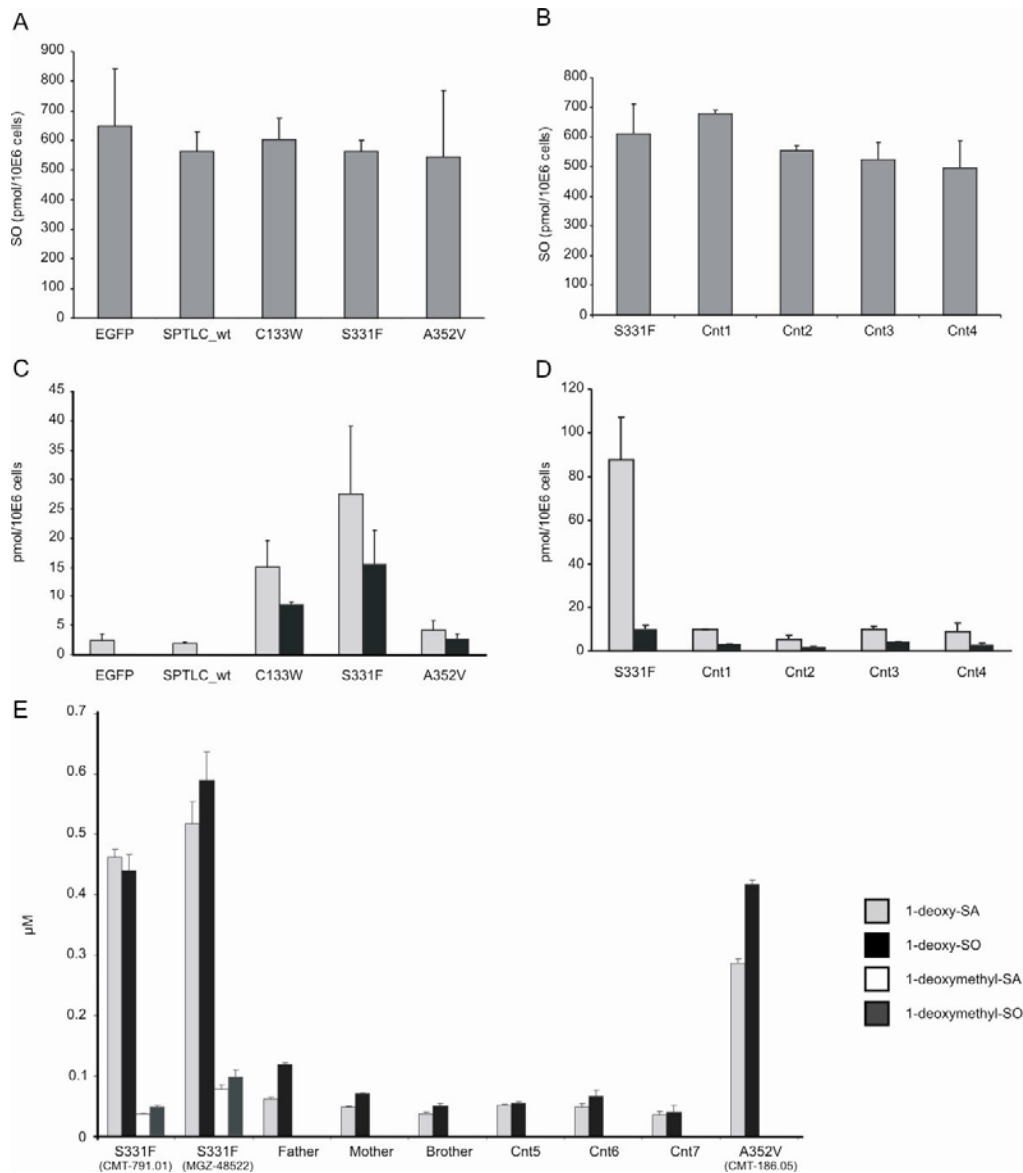


Figure 3. Levels of sphingosine and DSBs. (A,B) Levels of SO are measured after an acid and base hydrolysis assay on the extracted lipids in A. HEK293T cells and B. lymphoblast cells. (B) SO levels in a lymphoblast cell line of patient CMT-791.01 carrying the p.S331F mutation are compared to the levels in the unaffected parents (Cnt1 and Cnt2) and unrelated healthy controls (Cnt3 and Cnt4). (C,D) Levels of 1-deoxy-SA and 1-deoxy-SO are measured after an acid and base hydrolysis of the extracted lipids in C. HEK293T cells and D. lymphoblast cells. The levels in lymphoblast cell lines of patient CMT-791.01 with the p.S331F mutation are compared to the levels in the unaffected parents (Cnt1 and Cnt2) and unrelated healthy controls (Cnt3 and Cnt4). (E) DSB levels in plasma samples of p.S331F patient CMT-791.01, p.S331F patient MGZ-48522 and his unaffected family members (father, mother and brother), p.A352V patient CMT-186.05 and of three unrelated and healthy control individuals (Cnt5, Cnt6 and Cnt7). For each assay, a representative experiment is shown. Data is represented as a mean with error bars representing standard deviations. Standard deviation was calculated based on three independent experiments. SA: sphinganine; SO: sphingosine.

To explain the more severe phenotype in p.S331F patients, we compared the effect of the p.S331F mutation and the most intensively studied mutation associated with a typical HSAN-I phenotype, p.C133W, on SPT enzyme properties. Our results show that the p.S331F mutation lowers canonical SPT activity without reducing total

sphingolipid levels in HEK293T cells or patient lymphoblast cells. In addition, the DSB levels were highly elevated compared to wt cells, but not significantly different from the level observed in p.C133W expressing cells. In this context, it is important to mention that we were likewise unable to observe a correlation between DSB levels and the clinical phenotype in our previous study on HSAN-I causing *SPTLC2* mutations (Rotthier et al., 2010). This might imply that DSB levels are not correlated to the severity of the disease, but that other factors, such as genetic modifiers, modulate the clinical phenotype. Alternatively, the S331 amino acid might be involved in other, yet unidentified functions of the SPT complex that are changed upon mutation. As is apparent from the model of the human SPT structure (Fig. 1b), the S331 amino acid residue is located on the surface of the protein, rendering it possible that this residue is involved in the interaction with other proteins, such as the recently identified small stimulatory subunits of SPT (ssSPT) (Han et al., 2009) and ORM-like proteins (Breslow et al., 2010; Han et al., 2010). However, information on functional domains of the mammalian SPTLC1 subunit is still lacking, limiting the conclusions that can be drawn from the model.

The biochemical evidence reported so far indicates that all pathogenic mutants in *SPTLC1* and *SPTLC2* are consistently associated with a reduction in the canonical SPT activity and an increased formation of DSB (Eichler et al., 2009; Penno et al., 2010; Rotthier et al., 2010) (for overview: see Table 1). This is reinforced by the case of the p.G387A variant in *SPTLC1*. This variant was initially thought to cause HSAN-I in twin sisters (Verhoeven et al., 2004), but does not decrease SPT activity (Hornemann et al., 2009) nor increase DSB generation (unpublished data). It turned out to be a rare, benign SNP as it was found in homozygous state in a healthy individual (Hornemann et al., 2009). We used the information above to assess the impact of the p.A352V variant. Although the patient presents with a typical HSAN-I phenotype and despite the absence of the mutation from 300 control individuals, segregation analysis of the p.A352V mutation is lacking, the evolutionary conservation of the targeted amino acid is limited and the chemical properties of alanine and valine are similar, justifying caution in the interpretation of the genetic data. The biochemical experiments performed in this study strengthen the pathogenicity of this variant: it reduces SPT activity *in vitro* and is associated with accumulation of DSBs in plasma of the patient, but yet does not cause DSB accumulation in stably expressing HEK cells. A similar effect is seen for the p.V144D variant: it shows a clearly reduced SPT activity *in vitro* and significantly elevated DSB levels in plasma (Penno et al., 2010), but only slightly elevated DSB formation in stably expressing HEK cells (unpublished data). The reason for this discrepancy in DSB accumulation between stably transfected cells and plasma samples is unclear. One possibility is that the effect of the p.A352V and p.V144D mutations on the biochemical properties of SPT is more subtle than that of the other *SPTLC1* and *SPTLC2* mutations, leading to a slower rate of DSB formation. In HEK cells, that are allowed to produce DSBs over approximately 72 hours, DSB levels might not have reached the limit of detection, while the DSB levels in plasma reflect the long term accumulation in patients. However, since the plasma samples are physiologically more relevant, we conclude that the p.A352V mutation is indeed disease associated.

These results demonstrate the importance of analyzing patient material in addition to performing experiments on cell lines overexpressing the mutant protein. Furthermore, the consistent presence of DSBs in plasma shows that this could be a valuable biomarker for HSAN-I.

Analysis of plasma samples shows that the p.S331F mutation additionally increases the affinity of the SPT enzyme for glycine, an effect that was previously observed for the p.C133W mutation. The absence of increased levels of 1-deoxymethyl-SA in the plasma of patients with the mutation p.C133Y, p.V144D (Penno et al., 2010) or p.A352V (this study) indicates however that 1-deoxymethyl-SA is not essential for the pathogenesis of HSAN-I. Furthermore, the neurotoxic effect on primary sensory neurons was less pronounced with 1-deoxymethyl-SA than with 1-deoxy-SA (Penno et al., 2010). Nevertheless, a contributory role for 1-deoxymethyl-SA in the pathogenesis cannot be excluded at this point.

Table 1. Overview of all currently known SPTLC1 and SPTLC2 mutations and polymorphisms, the associated clinical features and biochemical characteristics

Variant	Disease characteristics		Biochemical characteristics		Ref
	Age at onset	Clinical features	SPT activity	DSB formation	
SPTLC1					
p.C133W (c.399T>G)	Adolesc – adult	Predominant SN, ulceromutilations, lancinating pains	↓	↑↑	Bejaoui 2001 & 2002; Dawkins 2001; Dedov 2004; Gable 2002; Hornemann 2009; McCampbell 2005; Penno 2010
p.C133Y (c.398G>A)	Adolesc – adult	Predominant SN, ulceromutilations, lancinating pains	↓	↑↑	Bejaoui 2001 & 2002; Dawkins 2001; Gable 2002; Penno 2010
p.C133R (c.397T>C)	Adult	Predominant SN	?	?	Rautenstrauss 2009
p.V144D (c.431T>A)	Adolesc - adult	Predominant SN, ulceromutilations, lancinating pains	↓	↑ (plasma)	Dawkins 2001; Gable 2002; Hornemann 2009; Penno 2010
p.S331F (c.992C>T)	Cong (CMT-791.01)	Insensitivity to pain, ulcerations, motor involvement, severe growth and mental retardation, microcephaly, hypotonia, vocal cord paralysis, gastro-oesophageal reflux	↓	↑↑	Rotthier 2009; this study
	Early onset (MGZ-48522)	Insensitivity to pain, ulcerations, motor impairment, juvenile cataract			this study
p.A352V (c.1055C>T)	16y	Predominant SN, lancinating pains, no ulceromutilations	↓	↑ (plasma)	Rotthier 2009; this study
p.G387A (c.1160G>C)	Not disease associated		-	-	Verhoeven 2004; Hornemann 2009
SPTLC2					
p.V359M (c.1075G>A)	52y	Predominant SN, ulceromutilations	↓	↑↑	Rotthier 2010
p.G382V (c.1145G>T)	adult	Predominant SN, ulceromutilations	↓	↑↑	Rotthier 2010
p.I504F (c.1510A>T)	5y	Sensory dysfunction, ulcerations and osteomyelitis, distal weakness, foot deformities, anhidrosis	↓	↑↑	Rotthier 2010

Y: years; Adolesc: adolescent; Cong: congenital; SN: sensory neuropathy; DSB: deoxysphingoid bases; ↓: reduced; ↑: moderately elevated; ↑↑: highly elevated; -: unchanged; ?: not assessed

The question of the causality in HSAN-I is subject of debate. The impact of reduced SPT activity on total sphingolipid levels remains controversial. Reports on decreased ceramide and sphingomyelin synthesis were published (Bejaoui et al., 2002; Gable et al., 2002), other studies reported increased levels of glucosylceramide (McCampbell et al., 2005), while yet other reports did not observe any changes in lipid composition (Dedov et al., 2004; Hornemann et al., 2007). In this study, we showed that total sphingolipid levels are not significantly altered by the reduction in canonical SPT activity (Fig 3a,b). In addition, heterozygous *SPTLC1* and *SPTLC2* knockout mice, despite showing significantly reduced SPT activity (Hojjati et al., 2005), do not develop a neuropathy even at older age, rendering it unlikely that haploinsufficiency itself is sufficient to cause HSAN-I. Toxicity inherent to the mutant protein is also unlikely to be the causative factor, since double transgenic mice overexpressing both wt *SPTLC1* and the p.C133W variant do not develop a neuropathy (Eichler et al., 2009). These observations strengthen the hypothesis that the accumulation of neurotoxic DSBs underlies the pathology in HSAN-I (Eichler et al., 2009; Penno et al., 2010). This is further supported by the observation that the exogenous addition of 1-deoxy-SA but not of SA to cultured primary dorsal root ganglia is neurotoxic by impairing neurite outgrowth, probably secondary to disturbing cytoskeletal integrity (Penno et al., 2010). In this context, it is interesting to note that exogenous addition of 1-deoxy-SA was reported earlier to impair stress fiber formation by interfering with the Rho GTPase signaling cascade (Cuadros et al., 2000). Members of the Rho GTPase family regulate various processes involving actin and neurofilament dynamics, cell polarization, axonal stabilization and growth cone formation (Heasman and Ridley, 2008). Destabilization of axonal structures could be envisaged to cause the progressive

axonal degeneration seen in HSAN-I patients. However, whether the endogenous generation of 1-deoxy-SA in neuronal cells has the same effect has not been investigated yet.

In conclusion, our results demonstrate that the SPTLC1 mutation p.S331F, which is associated with a severe HSAN-I phenotype, has the same effect on SPT activity and DSB formation as the previously characterized SPTLC1 mutations, suggesting that additional factors influence the disease course. Furthermore, we show that the p.A352V mutation, for which genetic evidence for pathogenicity is poor, is truly disease causing, as it is associated with a reduced SPT activity and elevated DSB levels in patient plasma.

ACKNOWLEDGMENTS

We are grateful to the patients for their contribution to this study. We thank N. Bonnelo for assistance in patient's management and J.-P. Timmermans for access to the microscopy facility at the University of Antwerp. This project was in part funded by a Methusalem grant of the University of Antwerp, the Fund for Scientific Research (FWO-Flanders), the Medical Foundation Queen Elisabeth (GSKE), the 'Association Belge contre les Maladies Neuromusculaires' (ABMM) and the Interuniversity Attraction Poles P6/43 program of the Belgian Federal Science Policy Office (BELSPO). A.R. is supported by a PhD fellowship of the Institute for Science and Technology (IWT). A.R. received an EMBO Short Term Fellowship. K.J. holds a postdoctoral fellowship from BELSPO. Support for H.T. was provided by the German Society for Clinical Chemistry and Laboratory Medicine (DGKL), the Gebert R uf Foundation and the European Commission (LSHM-CT-2006-037631).

REFERENCES

- Aboussouan LS, Lewis RA, Shy ME. 2007. Disorders of pulmonary function, sleep, and the upper airway in Charcot-Marie-Tooth disease. *Lung* 185:1-7.
- Auer-Grumbach M, De JP, Verhoeven K, Timmerman V, Wagner K, Hartung HP, Nicholson GA. 2003. Autosomal dominant inherited neuropathies with prominent sensory loss and mutilations: a review. *Arch Neurol* 60:329-334.
- Bejaoui K, Uchida Y, Yasuda S, Ho M, Nishijima M, Brown RH, Jr., Holleran WM, Hanada K. 2002. Hereditary sensory neuropathy type 1 mutations confer dominant negative effects on serine palmitoyltransferase, critical for sphingolipid synthesis. *J Clin Invest* 110:1301-1308.
- Bejaoui K, Wu C, Scheffler MD, Haan G, Ashby P, Wu L, de Jong P, Brown RH, Jr. 2001. SPTLC1 is mutated in hereditary sensory neuropathy, type 1. *Nat Genet* 27:261-262.
- Breslow DK, Collins SR, Bodenmiller B, Aebersold R, Simons K, Shevchenko A, Ejsing CS, Weissman JS. 2010. Orm family proteins mediate sphingolipid homeostasis. *Nature* 463:1048-1053.
- Claeys KG, Zuchner S, Kennerson M, Berciano J, Garcia A, Verhoeven K, Storey E, Merory JR, Bienfait HM, Lammens M, Nelis E, Baets J, De Vriendt E, Berneman ZN, De V, I, Vance JM, Nicholson G, Timmerman V, De Jonghe P. 2009. Phenotypic spectrum of dynamin 2 mutations in Charcot-Marie-Tooth neuropathy. *Brain* 132:1741-1752.
- Cuadros R, Montejo de GE, Wandosell F, Faircloth G, Fernandez-Sousa JM, Avila J. 2000. The marine compound spisulosine, an inhibitor of cell proliferation, promotes the disassembly of actin stress fibers. *Cancer Lett* 152:23-29.
- Dawkins JL, Hulme DJ, Brahmabhatt SB, Auer-Grumbach M, Nicholson GA. 2001. Mutations in SPTLC1, encoding serine palmitoyltransferase, long chain base subunit-1, cause hereditary sensory neuropathy type I. *Nat Genet* 27:309-312.
- Dedov VN, Dedova IV, Merrill AH, Jr., Nicholson GA. 2004. Activity of partially inhibited serine palmitoyltransferase is sufficient for normal sphingolipid metabolism and viability of HSN1 patient cells. *Biochim Biophys Acta* 1688:168-175.
- Dyck PJ, Chance P, Lebo R, Carney JA. 1993. Hereditary motor and sensory neuropathies. In: Dyck PJ, Thomas PK, Griffin JW, Low PA, Poduslo JF, editors. *Peripheral Neuropathy*. Philadelphia: W.B. Saunders Company. p 1094-1136.
- Eichler FS, Hornemann T, McCampbell A, Kuljis D, Penno A, Vardeh D, Tamrazian E, Garofalo K, Lee HJ, Kini L, Selig M, Frosch M, Gable K, von Eckardstein A, Woolf CJ, Guan G, Harmon JM, Dunn TM, Brown RH, Jr. 2009. Overexpression of the wild-type SPT1 subunit lowers desoxysphingolipid levels and rescues the phenotype of HSAN1. *J Neurosci* 29:14646-14651.

- Gable K, Gupta SD, Han G, Niranjankumari S, Harmon JM, Dunn TM. 2010. A disease-causing mutation in the active site of serine palmitoyltransferase causes catalytic promiscuity. *J Biol Chem* 285:22846-22852.
- Gable K, Han G, Monaghan E, Bacikova D, Natarajan M, Williams R, Dunn TM. 2002. Mutations in the yeast LCB1 and LCB2 genes, including those corresponding to the hereditary sensory neuropathy type I mutations, dominantly inactivate serine palmitoyltransferase. *J Biol Chem* 277:10194-101200.
- Han G, Gupta SD, Gable K, Niranjankumari S, Moitra P, Eichler F, Brown RH, Jr., Harmon JM, Dunn TM. 2009. Identification of small subunits of mammalian serine palmitoyltransferase that confer distinct acyl-CoA substrate specificities. *Proc Natl Acad Sci USA* 106:8186-8191.
- Han S, Lone MA, Schneider R, Chang A. 2010. Orm1 and Orm2 are conserved endoplasmic reticulum membrane proteins regulating lipid homeostasis and protein quality control. *Proc Natl Acad Sci USA* 107:5851-5856.
- Hanada K. 2003. Serine palmitoyltransferase, a key enzyme of sphingolipid metabolism. *Biochim Biophys Acta* 1632:16-30.
- Heasman SJ, Ridley AJ. 2008. Mammalian Rho GTPases: new insights into their functions from in vivo studies. *Nat Rev Mol Cell Biol* 9:690-701.
- Hojjati MR, Li Z, Jiang XC. 2005. Serine palmitoyl-CoA transferase (SPT) deficiency and sphingolipid levels in mice. *Biochim Biophys Acta* 1737:44-51.
- Hoofst RW, Vriend G, Sander C, Abola EE. 1996. Errors in protein structures. *Nature* 381:272.
- Hornemann T, Penno A, Richard S, Nicholson G, van Dijk FS, Rotthier A, Timmerman V, von Eckardstein A. 2009. A systematic comparison of all mutations in hereditary sensory neuropathy type I (HSAN I) reveals that the G387A mutation is not disease associated. *Neurogenetics* 10:135-143.
- Hornemann T, Wei Y, von Eckardstein A. 2007. Is the mammalian serine palmitoyltransferase a high-molecular-mass complex? *Biochem J* 405:157-164.
- Huehne K, Zweier C, Raab K, Odent S, Bonnaure-Mallet M, Sixou JL, Landrieu P, Goizet C, Sarlangue J, Baumann M, Eggermann T, Rauch A, Ruppert S, Stettner GM, Rautenstrauss B. 2008. Novel missense, insertion and deletion mutations in the neurotrophic tyrosine kinase receptor type 1 gene (NTRK1) associated with congenital insensitivity to pain with anhidrosis. *Neuromuscul Disord* 18:159-166.
- Indo Y, Tsuruta M, Hayashida Y, Karim MA, Ohta K, Kawano T, Mitsubuchi H, Tonoki H, Awaya Y, Matsuda I. 1996. Mutations in the TRKA/NGF receptor gene in patients with congenital insensitivity to pain with anhidrosis. *Nat Genet* 13:485-488.
- Kok C, Kennerson ML, Spring PJ, Ing AJ, Pollard JD, Nicholson GA. 2003. A locus for hereditary sensory neuropathy with cough and gastroesophageal reflux on chromosome 3p22-p24. *Am J Hum Genet* 73:632-637.
- Kolter T, Sandhoff K. 2006. Sphingolipid metabolism diseases. *Biochim Biophys Acta* 1758:2057-2079.
- McCampbell A, Truong D, Broom DC, Allchorne A, Gable K, Cutler RG, Mattson MP, Woolf CJ, Frosch MP, Harmon JM, Dunn TM, Brown RH, Jr. 2005. Mutant SPTLC1 dominantly inhibits serine palmitoyltransferase activity in vivo and confers an age-dependent neuropathy. *Hum Mol Genet* 14:3507-3521.
- Penno A, Reilly MM, Houlden H, Laura M, Rentsch K, Niederkofler V, Stoeckli ET, Nicholson G, Eichler F, Brown RH, Jr., von Eckardstein A, Hornemann T. 2010. Hereditary sensory neuropathy type 1 is caused by the accumulation of two neurotoxic sphingolipids. *J Biol Chem* 285:11178-11187.
- Rautenstrauss B, Neitzel B, Muench C, Haas J, Holinski-Feder E, Abicht A. 2009. Late onset hereditary sensory neuropathy type 1 (HSN1) is caused by a novel p.C133R missense mutation in SPTLC1. *J Periph Nerv Syst* 14(Supplement):124-125.
- Riley RT, Norred WP, Wang E, Merrill AH. 1999. Alteration in sphingolipid metabolism: bioassays for fumonisin- and ISP-I-like activity in tissues, cells and other matrices. *Nat Toxins* 7:407-414.
- Rotthier A, Baets J, De Vriendt E, Jacobs A, Auer-Grumbach M, Levy N, Bonello-Palot N, Kilic SS, Weis J, Nascimento A, Swinkels M, Kruyt MC, Jordanova A, De Jonghe P, Timmerman V. 2009. Genes for hereditary sensory and autonomic neuropathies: a genotype-phenotype correlation. *Brain* 132:2699-2711.

- Rotthier A, Auer-Grumbach M, Janssens K, Baets J, Penno A, Almeida-Souza L, Van Hoof K, Jacobs A, De Vriendt E, Schlotter-Weigel B, Loescher W, Vondracek P, Seeman P, De Jonghe P, Van Dijck P, Jordanova A, Hornemann T, Timmerman P. 2010. Mutations in the SPTLC2 subunit of serine palmitoyltransferase cause hereditary sensory and autonomic neuropathy type I. *Am J Hum Genet* 87:513-522.
- Rutti MF, Richard S, Penno A, von Eckardstein A, Hornemann T. 2009. An improved method to determine serine palmitoyltransferase activity. *J Lipid Res.* 50:1237-1244.
- Sánchez R, Sali A. 2000. Comparative protein structure modeling. Introduction and practical examples with modeller. *Methods Mol Biol.* 143:97-129.
- Salmon P, Trono D. 2002. Lentiviral vectors for the gene therapy of lympho-hematological disorders. *Curr Top Microbiol Immunol* 261:211-227.
- Sayle RA, Milner-White EJ. 1995. RASMOL: biomolecular graphics for all. *Trends Biochem Sci.* 20:374.
- Verhoeven K, Coen K, De Vriendt E, Jacobs A, Van Gerwen V, Smouts I, Pou-Serradell A, Martin JJ, Timmerman V, De Jonghe P. 2004. SPTLC1 mutation in twin sisters with hereditary sensory neuropathy type I. *Neurology* 62:1001-1002.
- Yard BA, Carter LG, Johnson KA, Overton IM, Dorward M, Liu H, McMahon SA, Oke M, Puech D, Barton GJ, Naismith JH, Campopiano DJ. 2007. The structure of serine palmitoyltransferase; gateway to sphingolipid biosynthesis. *J Mol Biol.* 370:870-886.
- Zitomer NC, Mitchell T, Voss KA, Bondy GS, Pruett ST, Garnier-Amblard EC, Liebeskind LS, Park H, Wang E, Sullards MC, Merrill AH, Jr., Riley RT. 2009. Ceramide synthase inhibition by fumonisin B1 causes accumulation of 1-deoxysphinganine: a novel category of bioactive 1-deoxysphingoid bases and 1-deoxydihydroceramides biosynthesized by mammalian cell lines and animals. *J Biol Chem* 284:4786-4795.

SUPP. MATERIALS AND METHODS

Lentiviral transduction of SH-SY5Y cells

Lentivirus encoding wt or mutant SPTLC1-EGFP fusion constructs was produced in HEK293T cells by cotransfection of 10 µg pLenti-SPTLC1 expression construct together with 3 µg of pMD2-VSV and 6.5 µg of pCMV-R8.91 viral packaging vectors for lentivirus. The calcium transfection medium was replaced 8 h posttransfection with medium containing 10 mM sodium butyrate to enhance promoter activity. The following day the medium was replaced with complete MEM medium and lentiviral production was allowed to proceed for 24 h. The produced lentivirus was harvested by filtering the supernatant.

Stable neuronal cell lines (SH-SY5Y) were obtained by lentiviral transduction, according to the method described by Salmon and Trono (Salmon and Trono, 2002). After infection, the cells were selected in complete MEM containing the selection agent blasticidin (3 µg/ml) for 2-3 weeks. The whole population of selected cells was pooled for further experiments.

Western blot

Cell lysates from stably expressing HEK293T cells were prepared in E1A lysis buffer (1% NP-40, 20 mM HEPES (pH 7.9), 250 mM NaCl, 20 mM β-glycerophosphate, 10 mM NaF, 1 mM sodium orthovanadate, 2 mM dithiothreitol, 1 mM EDTA and a protease inhibitor cocktail). Protein concentration was determined using the Bradford method (Biorad, Hercules, USA). Equal amounts of protein extracts were separated on 4-12% Bis-Tris NuPAGE gels (Invitrogen) and transferred to nitrocellulose membranes (HybondTM-P, GE Healthcare, Uppsala, Sweden). After blocking in 5% milk powder in PBS-Tween (1x PBS supplemented with 0.1% Tween 20), blots were incubated with a primary polyclonal SPTLC1 antibody (1:2500; BD Biosciences, Franklin Lakes, USA) overnight at 4°C, washed with PBS-Tween and incubated for one hour with a secondary horseradish peroxidase conjugated anti-mouse antibody (1:10000; GE healthcare). After washing, blots were developed using the enhanced chemiluminescence PlusTM detection system (GE healthcare).

Immunocytochemistry and microscopy

SH-SY5Y cells stably expressing EGFP-tagged wt or mutant SPTLC1 were fixed in 4% paraformaldehyde in PBS for 20 min, followed by a permeabilization step in 0.1% Triton X-100 in PBS for 3 min. After blocking with 5% FBS and 0.5% BSA in PBS-Triton (1x PBS supplemented with 0.02% Triton) for 1 h, cells were incubated with primary monoclonal antibody recognizing the ER marker calreticulin (1:500; Abcam, Cambridge, UK) for 1 h at room temperature. The primary antibody was detected using a secondary donkey anti-mouse IgG conjugated to Alexa Fluor 594 (1:200; Molecular Probes, Paisley, UK) for 1 h at room temperature, combined with Hoechst 33342 (Invitrogen) for staining of the nuclei. After washing with PBS, cells were mounted in Vectashield medium (Vector Labs, Burlingame, USA). Cells were microscopically examined and images were acquired on a Zeiss Axiovert 200 microscope with a microlens-enhanced dual spinning disc confocal system (UltraVIEW ERS; PerkinElmer, Seer Green, UK), equipped with a 60X 1.4 NA-objective.

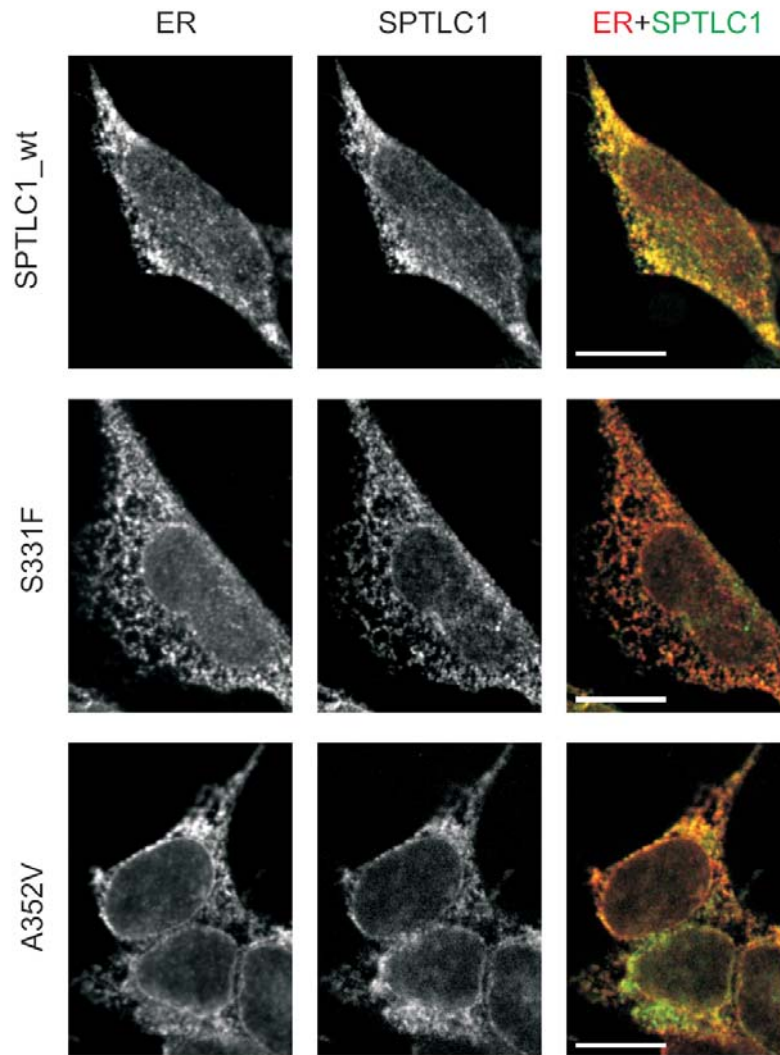
Supp. Table S1. Sequences of primers used for cloning and site-directed mutagenesis

Primer	Sequence (5'-3')
SPTLC1_attb1	ggggacaagttgtacaaaaagcaggctatggcgaccgccacggagcagtggg
SPTLC1_attb2	ggggaccactttgtacaagaaagctgggctcagcaggacggcctgggctac
SPTLC1_C133W_fw	gcgtggggacttggggaccagaggat
SPTLC1_C133W_rv	atcctctgggtcccaagtccccacgc
SPTLC1_S331F_fw	tgaattgaccatcagcacttttcggccaggata
SPTLC1_S331F_rv	tatcctggccgaaaagtcgctgatggtcaattaca
SPTLC1_A352V_fw	tgctgcagcaattgaggtcctcaacatcatggaag
SPTLC1_A352V_rv	cttccatgatgttgaggacctcaattgctcagca

Fw: forward; Rv: reverse



Supp. Figure S1. Expression of wt and mutant SPTLC1 in HEK293T cells. Western blot shows equal expression levels of endogenous SPTLC1 (lower band, 53 kDa) and V5-tagged SPTLC1 (upper band). Given the comparable intensity of the wt and mutant transgenic bands, it can be concluded that the mutations do not interfere with the expression of the protein. Moreover, this blot shows that the transgenes are expressed at a moderate level with an approximate 1 to 1 ratio of transgenic and endogenous SPTLC1, mimicking the situation in HSAN-I patients.



Supp. Figure S2. Confocal micrographs of SH-SY5Y cells expressing SPTLC1. Cells were transfected with either wt (upper row) or mutant EGFP-tagged SPTLC1 (middle and lower row; green in merge) and stained for endogenous calreticulin expression (red in merge) to study colocalization of wt and mutant protein with the ER. Scale bar = 10 μ m. The identical localization of V5-tagged and EGFP-tagged wild type SPTLC1 (data not shown) indicates that the EGFP-tag does not interfere with the localization of the protein. Wt EGFP-tagged SPTLC1 clearly colocalized with calreticulin, confirming that the EGFP-tag does not disturb the proper localization of the transgenic protein. Similarly to wt SPTLC1, both the p.S331F and the p.A352V mutants colocalized with calreticulin, showing that the mutations do not cause mislocalization of the mutant protein.